

DAMAGE MECHANICS BASED APPROACH IN FAILURE PREDICTION OF  
DRAW FORMING PROCESSES

ISMAIL BIN ABU SHAH

A thesis submitted in fulfilment of the  
requirements for the award of the degree of  
Doctor of Philosophy (Mechanical Engineering)

Faculty of Mechanical Engineering  
Universiti Teknologi Malaysia

JULY 2017

## **DEDICATION**

To my beloved parents and family

## ACKNOWLEDGEMENT

Praise to the Almighty.

First and foremost, thanks to Allah s.w.t for the continuous blessing and for giving me the strength and chances in completing this thesis. I would like to express my heartfelt appreciation to my respectful supervisor, Prof. Dr. Mohd. Nasir Tamin for his invaluable advice and supervision throughout this research.

Grateful acknowledgement is also made for financial support by the Ministry of Higher Education (MOHE) Malaysia and Universiti Teknikal Malaysia Melaka. This project is funded by the Ministry of Science, Technology and Innovation (MOSTI) Malaysia and Universiti Teknologi Malaysia through Grant No. TF0608C073-3H010 and RUG-00G42, respectively.

Apart from this, I am thankful to Computational Solid Mechanics Laboratory (CSMLab) members who have shared valuable information, knowledge and thought with me generously. It helps me to solve a lot of problems and difficulties. Their constructive ideas and opinions are also making this research a success indirectly.

Finally yet importantly, further gratitude is forwarded to my beloved family members and friends for their continuous supports and encouragements throughout these years.

## ABSTRACT

In a cup draw forming operation, the desired shape results from the material hardening process under controlled plastic deformation and the springback phenomena. In this study, a mechanics-of-deformation approach is developed based on damage variables and large plastic deformation. The approach is then employed to estimate the onset of the material damage event and the location of fracture based on the mechanics response of the metal blank. Draw forming behavior of low carbon steel is examined as a case study. The loading rate is conducted at a slow loading response of the steels in the large deformation of the draw forming processes. Axisymmetric and 3D solid models are developed for finite element (FE) simulations to gain insight into the evolution of internal states and damage in the steel blanks during the draw forming process. In the FE simulation, Johnson-Cook constitutive model with isotropic hardening rule is employed. The Rice-Tracey ductile damage criterion is employed to indicate damage initiation event along with a linear energy-displacement relation for damage evolution rule. Results show that while the applied loading (tool displacement) is quasi-static corresponding to the strain rate of  $0.001 \text{ sec}^{-1}$ , the maximum plastic strain rate at fracture could reach 100 times greater at the critical material flow region. Failure of the deforming steel blank is localized with excessive plastic deformation. While the onset of damage can be efficiently predicted using the axisymmetric FE model with damage-based model, the subsequent damage evolution of the localized ductile failure requires a 3D continuum FE model. The predicted tool load-displacement response is employed in validating the FE model. Effects of drawing parameters including drawing speed, blank holder force and die clearance on the resulting deformation of the drawn cup-shape part are established. Based on the response of the mechanics-of-deformation, the established failure prediction approach is proven more accurate and reliable.

## ABSTRAK

Di dalam operasi pembentukan cawan, bentuk yang diinginkan terhasil daripada proses pengerasan bahan di bawah fenomena tindakan ubah bentuk plastik dan anjalan. Di dalam kajian ini, kaedah mekanik ubah bentuk dibangunkan berdasarkan pemboleh ubah kerosakan dan ubah bentuk besar plastik. Kaedah ini kemudiannya diguna pakai bagi menganggarkan permulaan kejadian kerosakan bahan serta lokasi retakan berdasarkan tindak balas mekanik kepingan logam kosong. Sifat pembentukan keluli berkarbon rendah adalah dikaji sebagai satu kajian kes. Muatan ke besi dikenakan pada kadar tindak balas perlahan mengakibatkan perubahan besar dalam proses penghasilan pembentukan. Model asimetrik dan model pepejal 3D dibangunkan untuk simulasi unsur terhingga bagi mendapatkan pemahaman evolusi keadaan dalaman dan kerosakan logam kosong semasa proses pembentukan tarikan. Di dalam simulasi unsur terhingga, model menjuzuk Johnson-Cook bersama dengan peraturan pengerasan isotrop adalah diguna pakai. Kriteria kerosakan mulur Rice-Tracey digunakan bagi menunjukkan kejadian permulaan kerosakan berserta hubungan linear tenaga dan sesaran untuk peraturan evolusi kerosakan. Hasil menunjukkan walaupun laju alat yang dikenakan adalah pada kuasi-statik menurut kadar terikan  $0.001\text{saat}^{-1}$ , kadar terikan retakan plastik tertinggi boleh mencecah 100 kali ganda di kawasan genting pengaliran bahan. Kerosakan oleh perubahan logam kosong ditempatkan dengan lebihan ubah bentuk plastik. Sementara itu permulaan kerosakan boleh di jangka dengan berkesan menggunakan model simulasi unsur terhingga asimetrik menggunakan model berasaskan model kerosakan, evolusi kerosakan seterusnya adalah kerosakan mulur setempat memerlukan model unsur terhingga 3D. Jangkaan respon beban kepada sesaran digunakan bagi mengesahkan model simulasi unsur terhingga. Kesan parameter penarikan termasuk kelajuan penarikan, daya pemegang logam kosong dan kelegaannya acuan tekan pada hasil ubah bentuk oleh tertarik berbentuk cawan adalah tertubuh. Berdasarkan respon mekanik ubah bentuk, pendekatan jangkaan kerosakan tertubuh dibuktikan lebih tepat dan yakin.

## TABLE OF CONTENTS

| <b>CHAPTER</b> | <b>TITLE</b>                                | <b>PAGE</b> |
|----------------|---|-------------|
|                | <b>DECLARATION</b>                          | ii          |
|                | <b>DEDICATION</b>                           | iii         |
|                | <b>ACKNOWLEDGEMENT</b>                      | iv          |
|                | <b>ABSTRACT</b>                             | v           |
|                | <b>ABSTRAK</b>                              | vi          |
|                | <b>TABLE OF CONTENTS</b>                    | vii         |
|                | <b>LIST OF TABLES</b>                       | x           |
|                | <b>LIST OF FIGURES</b>                      | xi          |
|                | <b>LIST OF ABBREVIATIONS</b>                | xvi         |
|                | <b>LIST OF SYMBOLS</b>                      | xvii        |
| <b>1</b>       | <b>INTRODUCTION</b>                         | <b>1</b>    |
|                | 1.1 Background of the Study                 | 1           |
|                | 1.2 Statement of the Research Problem       | 3           |
|                | 1.3 Research Objectives                     | 3           |
|                | 1.4 Scope of the Study                      | 4           |
|                | 1.5 Significance of Study                   | 4           |
|                | 1.6 Thesis Layout                           | 5           |
| <b>2</b>       | <b>LITERATURE REVIEW</b>                    | <b>7</b>    |
|                | 2.1 Introduction                            | 7           |
|                | 2.2 Trends in Sheet Metal Forming Processes | 7           |
|                | Automotive Steel Sheets                     | 9           |
|                | 2.3 Formability in Draw Forming Processes   | 10          |
|                | Forming Limit Diagram                       | 11          |
|                | 2.4 Mechanics of Large Plastic Deformation  | 19          |

|          |  |           |
|----------|--|-----------|
| 2.5      | Strain Rate Dependent Models   | 26        |
|          | Johnson-Cook Model   | 27        |
| 2.6      | Continuum Damage Mechanics   | 28        |
|          | Damage Initiation Criterion  | 34        |
|          | Damage Evolution Equation  | 36        |
| 2.7      | Mechanisms of Failure  | 38        |
| 2.8      | FE Simulation of Sheet Metal Forming Processes                                   | 42        |
| 2.9      | Summary of Literature Review   | 49        |
| <b>3</b> | <b>RESEARCH METHODOLOGY</b>  | <b>52</b> |
| 3.1      | Introduction.  | 52        |
| 3.2      | Research Framework   | 57        |
| 3.3      | Demonstrator Material.   | 57        |
|          | Material Properties  | 57        |
|          | Properties and the Constitutive Model  | 59        |
|          | Material Damage Model  | 62        |
| 3.4      | Experimental Procedure.  | 64        |
|          | Erichsen Cup Forming Machine   | 64        |
| 3.5      | Finite Element Simulation of the Draw Forming Process                            | 66        |
|          | FE Circular Cup Draw Forming Model.  | 68        |
|          | Mesh Convergence Study   | 72        |
|          | Model Validation   | 74        |
| 3.6      | Concluding Remarks   | 76        |
| <b>4</b> | <b>DEFORMATION AND FAILURE PROCESSES IN DRAW FORMING OF A CIRCULAR CUP</b>       | <b>77</b> |
| 4.1      | Introduction   | 77        |
| 4.2      | Mechanics Deformation  | 78        |
| 4.3      | Effects of Blank Holder Force and Die Clearance Setting on Deformation Processes | 80        |
| 4.4      | Evolution of Plastic Instability.  | 84        |
| 4.5      | Fracture Location and Failure Mechanism  | 86        |

|          |     |   |            |
|----------|-----|---|------------|
|          | 4.6 | Summary   | 88         |
| <b>5</b> |     | <b>SIMPLIFIED OF FE SIMULATION OF THE DRAW FORMING PROCESS</b>          | <b>89</b>  |
|          | 5.1 | Introduction  | 89         |
|          | 5.2 | Characteristic of Stress and Strain Fields                              | 89         |
|          | 5.3 | Evolution of Plastic Instability  | 94         |
|          | 5.4 | Failure Mechanics   | 98         |
|          | 5.7 | Summary   | 98         |
| <b>6</b> |     | <b>FULL THREE DIMENSIONAL FE SIMULATION OF THE DRAW FORMING PROCESS</b> | <b>100</b> |
|          | 6.1 | Introduction  | 100        |
|          | 6.2 | Fracture Location   | 100        |
|          | 6.3 | Failure Mechanics   | 101        |
|          | 6.4 | Damage Initiation   | 103        |
|          | 6.5 | Damage Evolution  | 104        |
|          | 6.6 | Stress and Strain Behavior  | 106        |
|          | 6.7 | Characterization of Localized Thinning                                  | 107        |
|          | 6.8 | Fracture Propagation Path   | 109        |
|          | 6.9 | Summary   | 110        |
| <b>8</b> |     | <b>CONCLUSIONS &amp; RECOMMENDATIONS</b>                                | <b>112</b> |
|          | 7.1 | Conclusions   | 112        |
|          | 7.2 | Recommendations   | 113        |
|          |     | <b>REFERENCES</b>   | <b>114</b> |
|          |     | Appendices A - B  | 126-127    |



**LIST OF TABLES**

| <b>TABLE NO.</b> | <b>TITLE</b>  | <b>PAGE</b> |
|------------------|---|-------------|
| 2.1              | Three different deformation theories                          | 20          |
| 2.2              | Typical strain rates for various engineering problem          | 26          |
| 3.1              | Chemical composition of low carbon steel sheet (wt. %)        | 58          |
| 3.2              | Tensile properties at different strain rates                  | 60          |
| 3.3              | Elastic property and material density of LCS                  | 60          |
| 3.4              | Materials parameters used for J-C model                       | 61          |
| 3.5              | Combinations of process parameters for drawing cases examined | 65          |
| 5.1              | Interrupted sample test at various draw forming depth         | 94          |

## LIST OF FIGURES

| <b>FIGURE NO.</b> | <b>TITLE</b>   | <b>PAGE</b> |
|-------------------|--|-------------|
| 1.1               | Cross sectional view of typical cup draw forming process   | 2           |
| 2.1               | Trends of new material debut in every five years   | 8           |
| 2.2               | Relationship between ductility and tensile strength of various steel sheets  | 9           |
| 2.3               | Relationship between stress vs. percent elongation for various steel grades and their applications in auto-body structure        | 10          |
| 2.4               | Forming limit diagram  | 12          |
| 2.5               | Schematic representation of the strain path followed before and after necking  | 14          |
| 2.6               | An example of FFL on FLD plot  | 14          |
| 2.7               | M-K with the thickness imperfection method   | 16          |
| 2.8               | Deformation regimes in cup draw forming operation  | 22          |
| 2.9               | Diffused and localized necking phenomenon in thin sheet specimen   | 25          |
| 2.10              | Large plastic deformation covering elastic deformation, yielding, onset of diffused necking, onset of local necking and fracture | 25          |
| 2.11              | Analysis domains for solid mechanics   | 29          |
| 2.12              | Mechanical representation of damage  | 30          |
| 2.13              | Deformation and damage concept for mechanical equivalence of damage at mesoscale   | 32          |

|      |  |    |
|------|--|----|
| 2.14 | The concept for continuum damage mechanics   | 34 |
| 2.15 | Relationship between the equivalent strain with the stress triaxiality   | 35 |
| 2.16 | Damage evolution paths   | 37 |
| 2.17 | Mechanism of failure   | 39 |
| 2.18 | Damage process in different length scale   | 40 |
| 2.19 | Nucleation, growth and coalescence of microvoids   | 41 |
| 2.20 | Ductile failure behavior corresponding to the true stress strain   | 42 |
| 2.21 | A quarter of deformable blank illustrating the fracture in FLD post-processor  | 45 |
| 2.22 | Simulation results at different drawn depth with different stiffness degradation value compare to the experimental test                          | 46 |
| 2.23 | Simulation results prior to fracture at different drawn depth with different stiffness degradation   | 47 |
| 2.24 | Illustration of fracture in experiment and FE simulation corresponding to the FLD result and the load-displacement curve                         | 48 |
| 2.25 | Comparison between implicit and explicit integration domain  | 49 |
| 3.1  | Overall research methodology flow-chart  | 53 |
| 3.2  | Overall research methodology   | 54 |
| 3.3  | Microstructure of as received cold rolled 0.034C steel sheet (a) surface and (b) across thickness  | 59 |
| 3.4  | True stress-plastic strain curves at different strain rate   | 60 |
| 3.5  | Measured (solid lines) and predicted (dashed lines) true stress-plastic strain curves of 0.034C cold-drawn steel sheet at different strain rates | 62 |
| 3.6  | Damage initiation parameter for ductile failure  | 63 |

|      |  |    |
|------|--|----|
| 3.7  | Erichsen Cup Forming Machine   | 65 |
| 3.8  | Flow-chart of FE model setup with the preparation and model sensitivity analysis   | 67 |
| 3.9  | Physical model of circular cup shape part  | 68 |
| 3.10 | Schematic sectional view of forming tool design set-up for draw forming of cup-shape parts   | 69 |
| 3.11 | Boundary conditions of the draw forming process  | 70 |
| 3.12 | (a) Top view of meshed steel blank (b) compression and elongation region demonstrated in three-dimensional one over eight-size cup     | 71 |
| 3.13 | Sectional view of 3D draw forming model with boundary condition  | 72 |
| 3.14 | Mesh sensitivity analysis for selected region in the deformable blank  | 73 |
| 3.15 | Mesh sensitivity study conducted at the onset of fracture  | 74 |
| 3.16 | Comparison between measured and calculated tool force-displacement curve using axisymmetric model                                      | 75 |
| 3.17 | Comparison between measured and calculated tool force-displacement curve using 3D model  | 75 |
| 4.1  | Punch force-displacement curve illustrating the three stages of the steel blank deformation throughout the drawing process             | 80 |
| 4.2  | Variation of punch force with BHF and DC setting for sheet metal drawing of cup shape parts  | 81 |
| 4.3  | Variations of maximum drawing depth, $d_{max}$ and limit (non-damage) drawing depth, $d_L$ for sheet metal drawing of cup-shape parts. | 82 |
| 4.4  | Punch force-displacement curves at various DC settings for drawing case with BHF of 70 kN.   | 83 |
| 4.5  | Distance of fracture location at various DC setting at 70 kN of BHF.   | 84 |

|      |  |     |
|------|--|-----|
| 4.6  | Progressive thickness variation across necking band, shown at selected draw forming depth, case A11.                       | 85  |
| 4.7  | Evolution of necking during sheet metal drawing process for drawing case A11.  | 86  |
| 4.8  | Fracture locations.  | 87  |
| 4.9  | Fractured section of drawn cup for drawing case A11. Inset figure shows enlargement of the selected ductile failure area   | 87  |
| 4.10 | Characteristic of fractured surface at different BHF loading   | 88  |
| 5.1  | (a) Equivalent stress at draw forming depth of 10.7 mm (b) residual stress, (c) residual strain                            | 90  |
| 5.2  | Plastic strain rate measured at various locations  | 91  |
| 5.3  | Calculated strain rates at various location  | 93  |
| 5.4  | Evolution of necking during the sheet metal drawing process  | 95  |
| 5.5  | Thinning section along the blank profile   | 96  |
| 5.6  | The stress-strain behavior-along the profile   | 97  |
| 5.7  | Comparison between FE and experimental test with illustration of ductile failure.  | 98  |
| 6.1  | Comparison between the simulated FE and observed fracture location in the draw forming test                                | 101 |
| 6.2  | Comparison between FE and experimental draw forming test   | 102 |
| 6.3  | An element is separated from the cup sidewall at the onset of fracture   | 103 |
| 6.4  | Comparison between localized damage initiation variable and the global load-displacement response of the draw forming test | 104 |
| 6.5  | Degradation of critical element until it is separated  | 105 |
| 6.6  | Characteristic of stress and strain evolution throughout the draw forming process  | 106 |

|      |   |     |
|------|---|-----|
| 6.7  | Simulation results at several drawn depths of the interrupted draw forming                      | 107 |
| 6.8  | Comparison between FE simulations and experimental test of thru-thickness evolution             | 108 |
| 6.9  | Sectional view of fracture propagation from outer to inner fiber at various draw forming depths | 109 |
| 6.10 | Crack propagation of fracture in biaxial direction of fiber at different draw forming depth     | 110 |

## LIST OF ABBREVIATIONS

|      |   |                                   |
|------|---|-----------------------------------|
| AHSS | - | Advance High Strength Steel       |
| BHF  | - | Blank Holder Force                |
| CAE  | - | Computer Aided Engineering        |
| CDM  | - | Continuum Damage Mechanics        |
| Cof  | - | Coefficient of friction           |
| C-S  | - | Cowper- Symonds                   |
| DC   | - | Die Clearance                     |
| DIC  | - | Digital Image Correlation         |
| FE   | - | Finite Element                    |
| FFL  | - | Fracture Forming Limit            |
| FLC  | - | Forming Limit Curve               |
| FLD  | - | Forming Limit Diagram             |
| FLDF | - | Forming Limit Diagram at Fracture |
| FLDN | - | Forming Limit Diagram at Necking  |
| GTN  | - | Gurson–Tvergaard–Needleman        |
| HER  | - | Hole Expansion Ratio              |
| J-C  | - | Johnson-Cook                      |
| LCS  | - | Low Carbon Steel                  |
| LDH  | - | Limiting Dome Height              |
| LDR  | - | Limiting Drawing Ratio            |
| R-K  | - | Rusineck-Klapeczko                |
| RVE  | - | Representative Volume Element     |
| SEM  | - | Scanning Electron Microscope      |
| TM   | - | Tanimura-Mimura                   |
| Z-A  | - | Zerilli-Armstrong                 |

## LIST OF SYMBOLS

|                |   |  |
|----------------|---|--|
| $A$            | - | Area   |
| $A'$           | - | Johnson-Cook material constant                                 |
| $a$            | - | Material damage initiation parameters                          |
| $B'$           | - | Johnson-Cook strain hardening coefficient                      |
| $C'$           | - | Johnson-Cook strain rate sensitivity                           |
| $c$            | - | Material damage initiation parameters                          |
| $D$            | - | Damage variable  |
| $\dot{D}$      | - | Material constant  |
| $d$            | - | Drawing depth  |
| $d_i$          | - | Damage initiated   |
| $d_L$          | - | Drawing limit  |
| $d_{max}$      | - | Maximum drawing depth  |
| $dA$           | - | Change of area   |
| $dF$           | - | Change of loading force  |
| $d\sigma$      | - | Change of stress   |
| $d\varepsilon$ | - | Change of strain   |
| $E$            | - | Young's modulus  |
| $E_o$          | - | Young's modulus of the material in the initial undamaged state |
| $E_D$          | - | Damaged state after loading                                    |
| $F$            | - | Force  |
| $F_{max}$      | - | Maximum force  |
| $F_L$          | - | Limit punch force  |
| $G_f$          | - | Fracture energy  |
| $L$            | - | Characteristic length of the element                           |
| $m$            | - | Johnson-Cook temperature sensitivity                           |



|                            |   |   |
|----------------------------|---|---|
| $n$                        | - | Johnson-Cook strain hardening                                 |
| $T^*$                      | - | Johnson-Cook homologous temperature                           |
| $T_{melt}$                 | - | Melting temperature   |
| $T_{room}$                 | - | Room temperature  |
| $t$                        | - | Thickness   |
| $t_{blank}$                | - | Thickness of the blank  |
| $\bar{u}^{pl}$             | - | Equivalent plastic displacement                               |
| $\bar{u}_f^{pl}$           | - | Equivalent plastic displacement at failure (damage evolution) |
| $\nu$                      | - | Poisson's ratio   |
| $\omega_D$                 | - | Internal state variable                                       |
| $\Delta A$                 | - | Apparent area (undamaged surface)                             |
| $\Delta \tilde{A}$         | - | Changes the effective area                                    |
| $\Delta A_{void}$          | - | Area with micro-voids   |
| $\Delta F$                 | - | External loading force  |
| $\bar{\sigma}$             | - | Equivalent stress   |
| $\tilde{\sigma}$           | - | Effective stress  |
| $\sigma_m$                 | - | Mean stress   |
| $\sigma_y$                 | - | Yield stress  |
| $\sigma_{yo}$              | - | Value of yield stress when damage criterion is met            |
| $\varepsilon$              | - | Strain  |
| $\dot{\varepsilon}$        | - | Strain rate   |
| $\dot{\varepsilon}^*$      | - | Johnson-Cook dimensionless strain rate                        |
| $\dot{\varepsilon}_0$      | - | Johnson-Cook nominal strain rate                              |
| $\varepsilon_D^{pl}$       | - | Effective plastic strain at the damage initiation             |
| $\bar{\varepsilon}^{pl}$   | - | Equivalent plastic strain                                     |
| $\bar{\varepsilon}_0^{pl}$ | - | Effective plastic strain at the damage initiation             |
| $\bar{\varepsilon}_f^{pl}$ | - | Effective plastic strain at fracture                          |
| $\bar{\varepsilon}_D^p$    | - | Plastic strain rate at the onset of damage                    |

|                             |   |   |
|-----------------------------|---|---|
| $\dot{\bar{\epsilon}}^{pl}$ | - | Equivalent plastic strain during the damage evolution stage |
| $\eta$                      | - | Stress triaxiality  |
| $\rho$                      | - | Material density  |

**LIST OF APPENDICES**

| <b>APPENDIX.</b> | <b>TITLE</b>   | <b>PAGE</b> |
|------------------|--|-------------|
| A                | Mesh quality index for axisymmetric model of deformable blank. | 126         |
| B                | Mesh quality index for 3D model of deformable blank            | 127         |

## **CHAPTER 1**

### **INTRODUCTION**

#### **1.1 Background of Study**

Automotive body parts such as front quarter panel, suspension housing and floor panel are produced through numerous metal forming processes. It is a process of governing the formability of material into the desired shape throughout the forming operation without fail [1]. In the classical shop floor approach, the well-known forming limit diagram (FLD) is employed as a tool to predict the material failure in the metal forming operation. It is practiced as an approach to prevent the occurrence of fracture in sheet metal forming production.

In general, metal forming operation is divided into two main distinct processes, which are cutting and shaping. The process of cutting such as blanking is a process of separating the blank. While shaping for instance draw forming is to form the blank into desired parts. As the main shaping metal forming process in the automotive industries, the study of material failure concentrates on the draw forming operation. The typical tool and die movement are described thru the mechanism of the draw forming process. The tool consists of a punch, blank holder and die cavity while steel blank is employed as deformable parts as depicted in Figure 1.1. This monotonic loading process of punch draws the steel blank into the die cavity at a specified drawing depth and loading speed to draw forming shaped parts. The interactions between deformable blank and forming tools induced large plastic deformation until it is properly form into desired shape.

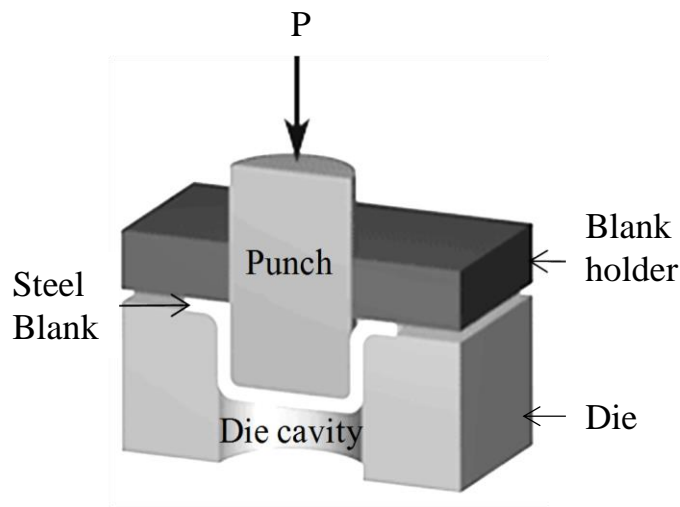


**Figure 0.1:** Cross sectional view of typical cup draw forming process

During the draw forming operation, steel blank undergoes material hardening process under controlled plastic deformation and springback phenomena. As a result, variation of thickness strain induced by the large plastic deformation is detected in the draw-forming cup. The blank holder force (BHF) induces the compressive stress at the flange region, while the punch tool induces the longitudinal and radial stresses throughout the loading process into the die cavity. These excessive stresses can cause the material failure known as wrinkling and localized necking. Wrinkling at flange is local buckling phenomena that attribute to the excessive compressive stresses [2]. Whereas, localized necking is due to the excessive tensile stresses [3]. The localized necking is usually detected in the sidewall region that can lead to ductile fracture.

As commonly practiced by the shop floor, the popular conventional FLD is defines as a linear strain path dependent criteria [4]. Thus, it is inaccurate for the analysis of complex draw forming processes [5]. The proposed approach is to use the internal states change of steel blank during draw forming processes. It is a mechanics of deformation approach. A process of degradation of material strength properties that initiate and evolve until fracture is dictated [6]. The failure prediction approach is developing based on the Rice-Tracey (R-T) ductile damage criterion to indicate the damage initiation event. While the linear energy-based relation, is used for damage evolution rule. The employ damage variables can estimate the localized deformation and tolerable stretching of material throughout the degradation process of material.

This mechanics of deformation approach is employed as a remedy to the problem in material failure prediction. The mechanics of deformation is a branch of mechanics that examines the behavior of material to the loading. It is an effort of investigating the non-linear response in the material due to the changes in geometry and internal state behavior throughout the draw forming operation.

## **1.2 Statement of the Research Problem**

How could the mechanics of deformation approach employing damage model and finite element (FE) simulation be used to predict material failure process in draw forming operation.

## **1.3 Objectives**

The aim of this study is to develop a damage-based failure prediction approach on the mechanics of materials deformation. Specific objectives are:

1. To establish a validated framework for FE simulation of draw forming processes.
2. To quantify the limitation of axisymmetric FE model for fracture.
3. To determine the effect of damage and its evolution on the material response.

## 1.4 Scope of Study

The present study covers the following scope of work:

1. Low carbon steel (LCS) is examined as a demonstrator material.
2. Erichsen cup forming machine is used to draw forming LCS into circular cup shape parts.
3. The draw forming test is set at 1 mm/sec slow loading rates with constant BHF to clamp uniformly on the flange part.
4. The FE simulations are carried out at strain rate dependent condition to model the draw forming test.
5. Coulomb friction is applied in every interaction between forming tools and deformable blank throughout the FE simulation.
6. Axisymmetric model with piecewise hardening curve is applied to define the limitation of the geometrical representation of the model when predicting failure.
7. Deformable blank in FE 3D circular cup is modeled using solid elements to determine the thru thickness necking effect.
8. Johnson-Cook (J-C) isotropic hardening parameter incorporated with Rice-Tracey (R-T) ductile damage initiation model and linear energy based model are used to assess hardening and material failure respectively.

## 1.5 Significance of Study

In predicting material failure, FLD shows some disadvantageous which requires new approach. Compared to the propose approach, its failure prediction quality is considered as inaccurate for the complex analysis of draw forming processes. This is due to its criteria that satisfy only for the linear strain path condition. Furthermore, it is highly depending on the recorded experimental test data with less mechanics based consideration. It is also very time consuming because it requires too

many data to be recorded with too many samples involved. As a result, these works suffered high in cost.

On the other hand, the propose failure prediction approach not only able to predict the onset of failure location accurately. Moreover, it is able to quantify the internal states of material from the process of thru thickness necking throughout the damage evolution until fracture. Therefore, the failure prediction results are more realistic compared to classical shop floor approach.

With the advance in numerical simulation to compute virtually the draw forming processes, the propose approach facilitates the assessment of deformation and failure. It computes the mechanics of deformation throughout the formability of material until the point of separation. Thru the understandings on mechanics of deformation and failure processes, the behavior of tolerable stretching of the material are define explicitly. It gives accurate and realistic physical representation of ductile failure at a localized point in the material.

## **1.6 Thesis Layout**

This thesis consists of seven chapters. In Chapter 1, the background and the necessity of the background of the research are bringing out. The issues of material failure in drawing automotive steel parts are based upon. The objectives, scope and significance of the research are present.

In Chapter 2, reviews are presented on the trends in sheet metal forming processes, automotive steel sheet, formability of draw forming processes, mechanics of large plastic deformation, finite element, strain rate dependent models, continuum damage mechanics, mechanism of failure, FE simulation of sheet metal forming processes and summary of literature review.



In Chapter 3, the research methodology is present. The details of the applied research materials, experimental setup and finite element (FE) simulation models are explained.

In Chapter 4, the assessment of deformation and failure processes in draw forming test are presented and discussed. Mechanics deformation of material formability through the punch-force displacement curve is examined and interpreted. Effects of BHF and DC setting in the process are measured. The interrupted draw forming tests at different displacement depth are conducted. The evolution of plastic instability in the interrupted draw-forming test is characterized. Fracture location and failure mechanism is identified.

In Chapter 5, the application of FE simulation to assess the mechanics deformation is addressed. An axisymmetric FE cup draw-forming model is used to simulate the draw forming processes on LCS at uniform BHF. In modeling the hardening behavior, piecewise plastic strain rate hardening parameter are employed. The evolution of plastic instability in the interrupted draw forming simulation is characterized. The calculated fracture location is compared.

In Chapter 6, the application of FE simulation to assess the damage mechanics is address. Using 3D FE cup model, the damage mechanics are examined by incorporating the J-C strain rate dependent criteria and damage variables until the event of fracture. The calculated localized thinning is characterized and compared. The fracture location in 3D FE cup model is demonstrated.

In Chapter 7, the major conclusions of the research are present. Future works for refining the research are recommend.

## REFERENCES

- [1] W. C. Emmens, *Formability*. Berlin, Heidelberg: Springer Berlin Heidelberg, 2011.
- [2] M. Kumar and A. Choudhary, "Plastic Wrinkling Investigation of Sheet Metal Product Made by Deep Forming Process: A FEM Study," *Int. J. Eng. Res. Technol.*, vol. 3, no. 10, pp. 186–191, 2014.
- [3] S. Patil and R. G. Tated, "Formability Analysis for Trapezoidal Cup Forming Using HyperForm," *Simul. Driven Innov.*, pp. 1–6, 2011.
- [4] M. Abbasi, M. A. Shafaat, M. Ketabchi, D. F. Haghshenas, and M. Abbasi, "Application of the GTN model to predict the forming limit diagram of IF-Steel," *J. Mech. Sci. Technol.*, vol. 26, no. 2, pp. 345–352, 2012.
- [5] S. J. Hashemi, H. M. Naeini, G. Liaghat, R. A. Tafti, and F. Rahmani, "Forming limit diagram of aluminum AA6063 tubes at high temperatures by bulge tests," *J. Mech. Sci. Technol.*, vol. 28, no. 11, pp. 4745–4752, 2014.
- [6] S. Murakami, *Continuum Damage Mechanics: Solid Mechanics and Applications*. Springer Berlin, 2012.
- [7] F. H. Aboutalebi, M. Farzin, and M. Mashayekhi, "Numerical Predictions and Experimental Validations of Ductile Damage Evolution," *Acta Mech. Solida Sin.*, vol. 25, no. 6, pp. 638–650, 2012.
- [8] O. J. Kwon, K. Y. Lee, G. S. Kim, and K. G. Chin, "New Trends in Advanced High Strength Steel Developments for Automotive Application," *Mater. Sci. Forum*, vol. 638–642, pp. 136–141, 2010.
- [9] Y. Abe, T. Ohmi, K. Mori, and T. Masuda, "Improvement of formability in deep drawing of ultra-high strength steel sheets by coating of die," *J. Mater. Process. Technol.*, vol. 214, no. 9, pp. 1838–1843, 2014.
- [10] H. Hayashi and T. Nakagawa, "Recent trends in sheet metals and their formability in manufacturing automotive panels," *J. Mater. Process. Technol.*, vol. 46, pp. 455–487, 1994.

- [11] M. Tisza, “Recent development trends in sheet metal forming,” *Int. J. Microstruct. Mater. Prop.*, vol. 8, no. 1/2, p. 125, 2013.
- [12] S. Coordinator and B. Sciences, “One day Symposium on Recent Trends and Advances in Sheet Metal Forming 1 st December 2012 Organized by One day Symposium on Recent Trends and Advances in Sheet Metal Forming Date :”
- [13] E. Dias, L. Horimoto, and M. dos Santos Pereira, “Microstructural Characterization of CP Steel Used in Automotive Industry,” *Mater. Sci. Forum*, vol. 775–776, pp. 141–145, 2014.
- [14] B. K. Zuidema, S. G. Denner, and B. Engl, “New High Strength Steels Applied to the Body Structure of ULSB\_AVC,” *SAE*, pp. 984–992, 2001.
- [15] S. L. Costa, J. P. Mendonça, and N. Peixinho, “Study on the impact behaviour of a new safety toe cap model made of ultra-high-strength steels,” *Mater. Des.*, vol. 91, pp. 143–154, 2016.
- [16] H. Tian, X. Liu, and J. Lin, “Investigation on the formability of tailor-welded blanks,” vol. 97–101, pp. 260–263, 2010.
- [17] S. Keeler, M. Kimchi, R. Kuziak, R. Kawalla, S. Waengler, and Y. G. Yuqing Weng, Han Dong, “Advanced high strength steels for automotive industry,” *Arch. Civ. Mech. Eng.*, vol. 8, no. 2, p. 511, 2014.
- [18] *Formability: A Review of Parameters and Processes that Control, Limit or Enhance the Formability of Sheet Metal*, vol. 7. 2011.
- [19] K. S. Prasad, T. Kamal, S. K. Panda, S. Kar, S. V. S. Narayana Murty, and S. C. Sharma, “Finite Element Validation of Forming Limit Diagram of IN-718 Sheet Metal,” *Mater. Today Proc.*, vol. 2, no. 4–5, pp. 2037–2045, 2015.
- [20] M. C. Butuc, a. Barata da Rocha, J. J. Gracio, and J. Ferreira Duarte, “A more general model for forming limit diagrams prediction,” *J. Mater. Process. Technol.*, vol. 125–126, pp. 213–218, 2002.
- [21] M. Bhargava, A. Tewari, and S. K. Mishra, “Forming limit diagram of Advanced High Strength Steels (AHSS) based on strain-path diagram,” *Mater. Des.*, vol. 85, pp. 149–155, 2015.
- [22] H. Kuramae, Y. Ikeya, H. Sakamoto, H. Morimoto, and E. Nakamachi, “Multi-scale parallel finite element analyses of LDH sheet formability tests based on crystallographic homogenization method,” *Int. J. Mech. Sci.*, vol. 52, no. 2, pp. 183–197, 2010.

- [23] K. Bandyopadhyay, S. K. Panda, P. Saha, and G. Padmanabham, "Limiting drawing ratio and deep drawing behavior of dual phase steel tailor welded blanks: FE simulation and experimental validation," *J. Mater. Process. Technol.*, vol. 217, pp. 48–64, 2015.
- [24] W. Wu, P. Zhang, X. Zeng, L. Jin, S. Yao, and A. A. Luo, "Bendability of the wrought magnesium alloy AM30 tubes using a rotary draw bender," *Mater. Sci. Eng. A*, vol. 486, no. 1–2, pp. 596–601, 2008.
- [25] S. K. Paul, M. Mukherjee, S. Kundu, and S. Chandra, "Prediction of hole expansion ratio for automotive grade steels," *Comput. Mater. Sci.*, vol. 89, pp. 189–197, 2014.
- [26] F. Ozturk, M. Dilmeç, M. Turkoz, R. E. Ece, and H. S. Halkacı, "Grid Marking and Measurement Methods for Sheet Metal Formability," *5th Int. Conf. Exhib. Des. Prod. Mach. Dies/Molds*, no. June, pp. 1–10, 2009.
- [27] K. Wang, J. E. Carsley, B. He, J. Li, and L. Zhang, "Journal of Materials Processing Technology Measuring forming limit strains with digital image correlation analysis," *J. Mater. Process. Technol.*, vol. 214, pp. 1120–1130, 2014.
- [28] H. J. Kim, S. C. Choi, K. T. Lee, and H. Y. Kim, "Experimental Determination of Forming Limit Diagram and Springback Characteristics of AZ31B Mg Alloy Sheets at Elevated Temperatures," *Mater. Trans.*, vol. 49, no. 5, pp. 1112–1119, 2008.
- [29] H. W. Swift, "Plastic instability under plane stress," *J. Mech. Phys. Solid*, vol. 1, pp. 1–18, 1952.
- [30] R. Hill, "on Discontinuous Reference Plastic States, With Special To Localized Necking in Thin Sheets," vol. 1, pp. 19–30, 1952.
- [31] L. Xue, "Localization conditions and diffused necking for damage plastic solids," *Eng. Fract. Mech.*, vol. 77, no. 8, pp. 1275–1297, 2010.
- [32] Y. Bouktir, H. Chalal, M. Haddad, and F. Abed-Meraim, "Investigation of ductility limits based on bifurcation theory coupled with continuum damage mechanics," *Mater. Des.*, vol. 90, pp. 969–978, 2016.
- [33] M. B. Silva, A. J. Martínez-Donaire, G. Centeno, D. Morales-Palma, C. Vallellano, and P. A. F. Martins, "Recent Approaches for the Determination of Forming Limits by Necking and Fracture in Sheet Metal Forming," *Procedia*

- Eng.*, vol. 132, no. January 2016, pp. 342–349, 2015.
- [34] J. M. Jalinier, “Calculation of the forming limit curve at fracture,” *J. Mater. Sci.*, vol. 18, no. 6, pp. 1794–1802, 1983.
- [35] P. M. Parmar and P. Ashish, “Comparative Study of Forming Limit Diagram for AISI 1020 Department of Mechanical ( Machine Design ),” vol. 3, no. 03, pp. 2822–2825, 2015.
- [36] D. Vysochinskiy, T. Coudert, O. S. Hopperstad, O. G. Lademo, and A. Reyes, “Experimental detection of forming limit strains on samples with multiple local necks,” *J. Mater. Process. Technol.*, vol. 227, pp. 216–226, 2016.
- [37] K. Isik, M. B. Silva, A. E. Tekkaya, and P. A. F. Martins, “Journal of Materials Processing Technology Formability limits by fracture in sheet metal forming,” *J. Mater. Process. Tech.*, vol. 214, no. 8, pp. 1557–1565, 2014.
- [38] M. He, F. Li, and Z. Wang, “Forming limit stress diagram prediction of aluminum alloy 5052 based on GTN model parameters determined by in situ tensile test,” *Chinese J. Aeronaut.*, vol. 24, no. 3, pp. 378–386, 2011.
- [39] H. Badreddine, C. Labergère, and K. Saanouni, “Ductile damage prediction in sheet and bulk metal forming,” *Comptes Rendus - Mec.*, vol. 344, no. 4–5, pp. 296–318, 2016.
- [40] Z. Marciniak, K. Kuczynski, and S. K. I. Warsaw, “N \_ N,” vol. 9, pp. 609–620, 1967.
- [41] M. Nurcheshmeh and D. E. Green, “Prediction of sheet forming limits with Marciniak and Kuczynski analysis using combined isotropicnonlinear kinematic hardening,” *Int. J. Mech. Sci.*, vol. 53, no. 2, pp. 145–153, 2011.
- [42] J. Slota, “Comparison of the forming - limit diagram (FLD) models for drawing quality (DQ) steel sheets,” *Metalurgija*, vol. 44, pp. 249–253, 2005.
- [43] K. Takuda, H. Mori, K. Takakura, N. Yamaguchi, “Finite element analysis of limit strain in biaxial stretching of sheet metals allowing ductile fracture,” *Int. J. Mech. Sci.*, vol. 42, pp. 785–798, 2000.
- [44] D. Banabic, “A review on recent developments of Marciniak-Kuczynski model,” *Comput. Methods Mater. Sci.*, no. 1952, pp. 1–24, 2010.
- [45] X. H. Hu, D. S. Wilkinson, M. Jain, P. D. Wu, and R. K. Mishra, “The impact of particle distributions and grain-level inhomogeneities on post-necking deformation and fracture in AA5754 sheet alloys during uniaxial tension,”

- Mater. Sci. Eng. A*, vol. 528, no. 4–5, pp. 2002–2016, 2011.
- [46] L. Leotoing and D. Guines, “Investigations of the effect of strain path changes on forming limit curves using an in-plane biaxial tensile test Investigations of the effect of strain path changes on forming limit curves using an in-plane biaxial tensile test,” vol. 99, pp. 21–28, 2015.
- [47] F. Ozturk and D. Lee, “Analysis of forming limits using ductile fracture criteria,” *J. Mater. Process. Technol.*, vol. 147, no. 3, pp. 397–404, 2004.
- [48] B. Li, T. J. Nye, and P. D. Wu, “Predicting the forming limit diagram of AA 5182-O,” *J. Strain Anal. Eng. Des.*, vol. 45, no. 4, pp. 255–273, 2010.
- [49] L. E. Bryhni D??hli, T. B??rvik, and O. S. Hopperstad, “Influence of loading path on ductile fracture of tensile specimens made from aluminium alloys,” *Int. J. Solids Struct.*, vol. 88–89, pp. 17–34, 2016.
- [50] F. A. McClintock, “A Criterion for Ductile Fracture by the Growth of Holes,” *J. Appl. Mech.*, vol. 35, no. 2, p. 363, 1968.
- [51] J. R. Rice and D. M. Tracey, “On the ductile enlargement of voids in triaxial stress fields,” *J. Mech. Phys. Solids*, vol. 17, no. 3, pp. 201–217, 1969.
- [52] G. Vadillo, J. Reboul, and J. Fernández-Sáez, “A modified Gurson model to account for the influence of the Lode parameter at high triaxialities,” *Eur. J. Mech. A/Solids*, vol. 56, pp. 31–44, 2016.
- [53] B. Ma, Z. G. Liu, Z. Jiang, X. Wu, K. Diao, and M. Wan, “Prediction of forming limit in DP590 steel sheet forming: An extended fracture criterion,” *Mater. Des.*, vol. 96, pp. 401–408, 2016.
- [54] M. V. Jr., P. A. Muñoz-Rojas, E. L. Cardoso, and M. Tomiyama, “Considerations on parameter identification and material response for Gurson-type and Lemaitre-type constitutive models,” *Int. J. Mech. Sci.*, vol. 106, pp. 254–265, 2016.
- [55] F. Xue, F. Li, B. Chen, J. Fan, and R. Wang, “A ductile-brittle fracture model for material ductile damage in plastic deformation based on microvoid growth,” *Comput. Mater. Sci.*, vol. 65, pp. 182–192, 2012.
- [56] V. Tvergaard, “Influence of Voids on Shear Band Instability Under Plane Strain Conditions,” *Int. J. Fract.*, vol. 17, no. 4, pp. 389–407, 1981.
- [57] V. Tvergaard and A. Needleman, “Analysis of the Cup-Cone Round Tensile Fracture,” *Acta Metall.*, vol. 32, no. I, pp. 157–169, 1984.

- [58] Z. Wang, A. Chapius, and Q. Liu, "Simulation of mechanical behavior of AZ31 magnesium alloy during twin-dominated large plastic deformation," *Trans. Nonferrous Met. Soc. China*, vol. 25, no. 11, pp. 3595–3603, 2015.
- [59] D. Brokken, W. A. M. Brekelmans, and F. P. T. Baaijens, "Numerical modelling of the metal blanking process," *J. Mater. Process. Technol.*, vol. 83, no. 83, pp. 192–199, 1998.
- [60] V. Lemiale, J. Chambert, and P. Picart, "Description of numerical techniques with the aim of predicting the sheet metal blanking process by FEM simulation," *J. Mater. Process. Technol.*, vol. 209, no. 5, pp. 2723–2734, 2009.
- [61] G. Eshel, M. Barash, and W. Johnson, "Rule based modeling for planning axisymmetrical deep-drawing," *J. Mech. Work. Technol.*, vol. 14, no. 1, pp. 1–115, 1986.
- [62] V. Vorkov, R. Aereus, D. Vandepitte, and J. R. Duflou, "Springback prediction of high-strength steels in large radius air bending using finite element modeling approach," *Procedia Eng.*, vol. 81, no. October, pp. 1005–1010, 2014.
- [63] E. H. Ouakdi, R. Louahdi, D. Khirani, and L. Tabourot, "Evaluation of springback under the effect of holding force and die radius in a stretch bending test," *Mater. Des.*, vol. 35, pp. 106–112, 2012.
- [64] B. Logue, M. Dingle, and J. L. Duncan, "Side-wall thickness in draw die forming," *J. Mater. Process. Technol.*, vol. 182, no. 1–3, pp. 191–194, 2007.
- [65] D. Chang, "An analytical model of the ironing process including redundant work effect," vol. 75, pp. 253–258, 1998.
- [66] S. Candra, I. M. L. Batan, W. Berata, and A. S. Pramono, "Analytical Study and FEM Simulation of the Maximum Varying Blank Holder Force to Prevent Cracking on Cylindrical Cup Deep Drawing," *Procedia CIRP*, vol. 26, pp. 548–553, 2015.
- [67] L. Zhong-qin, W. Wu-rong, and C. Guan-long, "A new strategy to optimize variable blank holder force towards improving the forming limits of aluminum sheet metal forming," *J. Mater. Process. Technol.*, vol. 183, no. 2–3, pp. 339–346, 2007.
- [68] J. Chen, X. Zhou, and J. Chen, "Sheet metal forming limit prediction based on plastic deformation energy," *J. Mater. Process. Technol.*, vol. 210, no. 2, pp. 315–322, 2010.

- [69] K. Osakada, "History of plasticity and metal forming analysis," *J. Mater. Process. Technol.*, vol. 210, no. 11, pp. 1436–1454, 2010.
- [70] Y. Ling, "Uniaxial true stress-strain after necking," *AMP J. Technol.*, vol. 5, no. 1, pp. 37–48, 1996.
- [71] J. Jeschke, D. Ostermann, and R. Krieg, "Critical strains and necking phenomena for different steel sheet specimens under uniaxial loading," *Nucl. Eng. Des.*, vol. 241, no. 6, pp. 2045–2052, 2011.
- [72] Y. Bao and T. Wierzbicki, "On fracture locus in the equivalent strain and stress triaxiality space," *Int. J. Mech. Sci.*, vol. 46, no. 1, pp. 81–98, 2004.
- [73] G. Mirone, "A new model for the elastoplastic characterization and the stress-strain determination on the necking section of a tensile specimen," *Int. J. Solids Struct.*, vol. 41, no. 13, pp. 3545–3564, 2004.
- [74] Z. L. Zhang, M. Hauge, J. Ødegård, and C. Thaulow, "Determining material true stress–strain curve from tensile specimens with rectangular cross-section," *Int. J. Solids Struct.*, vol. 36, no. 23, pp. 3497–3516, 1999.
- [75] Sing C. Tang and Jwo Pan, *Mechanics Modeling of Sheet Metal Forming*. SAE International, 2007.
- [76] S. Tanimura, T. Tsuda, A. Abe, H. Hayashi, and N. Jones, "Comparison of Rate-Dependent Constitutive Models with Experimental Data," *Int. J. Impact Eng.*, vol. 69, no. 0, pp. 104–113, 2014.
- [77] M. Dunand, "Effect of strain rate on the ductile fracture of Advanced High Strength Steel Sheets: Experiments and modeling," vol. 56, p. 236, 2013.
- [78] A. Reyes, O. S. Hopperstad, O. G. Lademo, and M. Langseth, "Modeling of textured aluminum alloys used in a bumper system: Material tests and characterization," *Comput. Mater. Sci.*, vol. 37, no. 3, pp. 246–268, 2006.
- [79] S. K. Paul, A. Raj, P. Biswas, G. Manikandan, and R. K. Verma, "Tensile flow behavior of ultra low carbon, low carbon and micro alloyed steel sheets for auto application under low to intermediate strain rate," *Mater. Des.*, vol. 57, pp. 211–217, 2014.
- [80] I. Rohr, H. Nahme, and K. Thoma, "Material characterization and constitutive modelling of ductile high strength steel for a wide range of strain rates," *Int. J. Impact Eng.*, vol. 31, no. 4, pp. 401–433, 2005.
- [81] G.R. Johnson and W.H. Cook, "A constitutive model and data for metals



- subjected to large strains, high strain rates and high temperatures.pdf,” in *Proceedings of the Seventh Symposium on Ballistics, The Hague, The Netherlands*, 1983, pp. 541–547.
- [82] L. Gambirasio and E. Rizzi, “An enhanced Johnson-Cook strength model for splitting strain rate and temperature effects on lower yield stress and plastic flow,” *Comput. Mater. Sci.*, vol. 113, pp. 231–265, 2016.
- [83] L. Gambirasio and E. Rizzi, “On the calibration strategies of the Johnson-Cook strength model: Discussion and applications to experimental data,” *Mater. Sci. Eng. A*, vol. 610, pp. 370–413, 2014.
- [84] I. Irausquín, J. L. Pérez-Castellanos, V. Miranda, and F. Teixeira-Dias, “Evaluation of the effect of the strain rate on the compressive response of a closed-cell aluminium foam using the split Hopkinson pressure bar test,” *Mater. Des.*, vol. 47, pp. 698–705, 2013.
- [85] F. Wang, J. Zhao, N. Zhu, and Z. Li, “A comparative study on Johnson-Cook constitutive modeling for Ti-6Al-4V alloy using automated ball indentation (ABI) technique,” *J. Alloys Compd.*, vol. 633, pp. 220–228, 2015.
- [86] R. J. Bhatt, “FLD Creation for SS304 Using Experiments and It ’ s Validation Using HyperForm 11.0,” no. 1946, pp. 1–6.
- [87] M. Turkoz, O. Yigit, M. Dilmeç, and H. S. Halkacı, “Construction of Forming Limit Diagram for AA 5754 and AA 2024 Aluminium Alloy,” in *Proceedings of the 12th International Conference on Aluminium Alloy*, 2010, pp. 516–521.
- [88] P. Teixeira, a. D. Santos, J. M. a. C. Sá, F. M. Andrade Pires, and a. B. Rocha, “Sheet metal formability evaluation using continuous damage mechanics,” *Int. J. Mater. Form.*, vol. 2, no. S1, pp. 463–466, 2009.
- [89] C. O. Arun, B. N. Rao, and S. M. Srinivasan, “Continuum damage growth analysis using element free Galerkin method,” *Sadhana - Acad. Proc. Eng. Sci.*, vol. 35, no. 3, pp. 279–301, 2010.
- [90] M. N. Tamin and N. M. Shaffiar, *Solder Joint Reliability Assessment: Finite Element Simulation Methodology*. Springer Science & Business, 2014.
- [91] J. Lin, M. Mohamed, D. Balint, and T. Dean, “The development of continuum damage mechanics-based theories for predicting forming limit diagrams for hot stamping applications,” *Int. J. Damage Mech.*, vol. 23, no. 5, pp. 684–701, 2013.

- [92] F. H. Aboutalebi, M. Farzin, and M. Mashayekhi, "Numerical Predictions and Experimental Validations of Ductile Damage Evolution," *Acta Mech. Solida Sin.*, vol. 25, no. 6, pp. 638–650, 2012.
- [93] *Advances in Applied Mechanics, Volume 27*. Academic Press, 1990.
- [94] Y. Lou, H. Huh, S. Lim, and K. Pack, "New ductile fracture criterion for prediction of fracture forming limit diagrams of sheet metals," *Int. J. Solids Struct.*, vol. 49, no. 25, pp. 3605–3615, 2012.
- [95] V. Uthaisangskuk, S. Muenstermann, U. Prahl, W. Bleck, H. P. Schmitz, and T. Pretorius, "A study of microcrack formation in multiphase steel using representative volume element and damage mechanics," *Comput. Mater. Sci.*, vol. 50, no. 4, pp. 1225–1232, 2011.
- [96] Vuong Nguyen Van Do, "The Behavior of Ductile Damage Model on Steel Structure Failure," vol. 142, p. 8, 2016.
- [97] J. Lian, H. Yang, N. Vajragupta, S. Muenstermann, and W. Bleck, "A method to quantitatively upscale the damage initiation of dual-phase steels under various stress states from microscale to macroscale," *Comput. Mater. Sci.*, vol. 94, no. C, pp. 245–257, 2014.
- [98] L. Kang, H. Ge, and X. Fang, "An improved ductile fracture model for structural steels considering effect of high stress triaxiality," vol. 115, pp. 634–650, 2016.
- [99] D. Chae and D. A. Koss, "Damage accumulation and failure of HSLA-100 steel," *Mater. Sci. Eng. A*, vol. 366, no. 2, pp. 299–309, 2004.
- [100] X. W. Chen, G. Chen, and F. J. Zhang, "Deformation and failure modes of soft steel projectiles impacting harder steel targets at increasing velocity," *Exp. Mech.*, vol. 48, no. 3, pp. 335–354, 2008.
- [101] H. Hooputra, H. Gese, H. Dell, and H. Werner, "A comprehensive failure model for crashworthiness simulation of aluminium extrusions," *Int. J. Crashworthiness*, vol. 9, no. 5, pp. 449–464, 2004.
- [102] Y. Bao and T. Wierzbicki, "On the cut-off value of negative triaxiality for fracture," *Eng. Fract. Mech.*, vol. 72, no. 7, pp. 1049–1069, 2005.
- [103] Abaqus, *Abaqus Analysis User's Manual*. Dassault Systemes Simulia Corp. RI, 2015.
- [104] M. Kurumatani, K. Terada, J. Kato, T. Kyoya, and K. Kashiyaama, "An isotropic damage model based on fracture mechanics for concrete," *Eng. Fract. Mech.*,

- vol. 155, pp. 49–66, 2016.
- [105] J. Lemaitre, “Coupled elasto-plasticity and damage constitutive equations,” *Comput. Methods Appl. Mech. Eng.*, vol. 51, pp. 31–49, 1985.
- [106] L. Zymbell, G. Hütter, T. Linse, U. Mühlich, and M. Kuna, “Size effects in ductile failure of porous materials containing two populations of voids,” *Eur. J. Mech. A/Solids*, vol. 45, pp. 8–19, 2014.
- [107] M. J. Nemcko, J. Li, and D. S. Wilkinson, “Effects of void band orientation and crystallographic anisotropy on void growth and coalescence,” vol. 95, pp. 270–283, 2016.
- [108] F. Liao, W. Wang, and Y. Chen, “Ductile fracture prediction for welded steel connections under monotonic loading based on micromechanical fracture criteria,” *Eng. Struct.*, vol. 94, pp. 16–28, 2015.
- [109] A. G. Leacock, “The Future of Sheet Metal Forming Research,” *Mater. Manuf. Process.*, vol. 27, no. 4, pp. 366–369, 2012.
- [110] T.-C. Hsu and C.-H. Chu, “A finite-element analysis of sheet metal forming processes,” *J. Mater. Process. Technol.*, vol. 54, no. 1–4, pp. 70–75, 1995.
- [111] S. Bruschi, T. Altan, D. Banabic, P. F. Bariani, A. Brosius, J. Cao, A. Ghiotti, M. Khraisheh, M. Merklein, and A. E. Tekkaya, “Testing and modelling of material behaviour and formability in sheet metal forming,” *CIRP Ann. - Manuf. Technol.*, vol. 63, no. 2, pp. 727–749, 2014.
- [112] K. Roll, “Simulation of sheet metal forming - Necessary developments in the future,” *Numisheet 2008*, no. September, pp. 59–68, 2008.
- [113] W. Wang, Y. Zhao, Z. Wang, M. Hua, and X. Wei, “A study on variable friction model in sheet metal forming with advanced high strength steels,” *Tribol. Int.*, vol. 93, pp. 17–28, 2015.
- [114] A. E. Tekkaya, “State-of-the-art of simulation of sheet metal forming,” *J. Mater. Process. Technol.*, vol. 103, no. 1, pp. 14–22, 2000.
- [115] V. Diviné, E. Beauchesne, Q. Zeng, M. Istrate, S. Roy, A. D. France, D. Renaissance, A. D. France, and D. Renaissance, “Failure Criteria for Stamping Analysis in Radioss,” 2014.
- [116] J. P. Fan, C. Y. Tang, C. P. Tsui, L. C. Chan, and T. C. Lee, “3D finite element simulation of deep drawing with damage development,” *Int. J. Mach. Tools Manuf.*, vol. 46, no. 9, pp. 1035–1044, 2006.

- [117] M. Khelifa, M. Oudjene, and A. Khennane, "Fracture in sheet metal forming: Effect of ductile damage evolution," *Comput. Struct.*, vol. 85, no. 3–4, pp. 205–212, 2007.
- [118] M. Goelke, "Practical Aspects of Finite Element Simulation – A Student Guide," p. 453, 2012.
- [119] P. Reddy, G. Reddy, and P. Prasad, "A Review on Finite Element Simulations in Metal Forming," *Ijmer.Com*, vol. 2, no. 4, pp. 2326–2330, 2012.
- [120] K.-J. Bathe, "On the State of Finite Element Procedures for Forming Processes," *Proc. 8th Int. Conf. Numer. Methods Ind. Form. Process.*, vol. 712, pp. 34–38, 2004.
- [121] T. Irie, S. Satoh, K. Hashiguchi, and I. Takahashi, "Metallurgical of Cold-rolled Affecting Strength Steel Formability Sheets," *Trans. ISIJ*, vol. 21, no. 793, pp. 793–801, 1981.
- [122] Paul S. Gupton, "A Practical Approach to Understanding Steels, Their Alloying, Heat Treatment and Surface Hardening," in *Proceedings of the Fourteenth Turbomachinery Symposium*, 1985, p. 103.
- [123] S. S. Arsad, "Unified Constitutive Models for Deformation of Thin-Walled Structures," Universiti Teknologi Malaysia, 2012.
- [124] M. N. Tamin, A. Abdul-Latif, A. Ayob, N. Kamsah, Y. Prawoto, Z. Ahmad, S. Abdullah, and A. Desa, "Damage and Fracture Mechanics-Based Design Methodology: Constitutive and Damage Models for Steel Sheet Metals.," in *Computationally Optimised Fuel-Efficient Concept Car (Vol.1)*, 2011, p. 38.
- [125] G. Fang\*, P. Zeng, and L. Lou, "Finite element simulation of effect of part shape on forming quality in fine-blanking process," *Procedia Eng.*, vol. 81, pp. 1108–1113, 2014.
- [126] N. S. Gokhale, *Practical Finite Element Analysis*. Finite To Infinite, 2008.
- [127] G. C. M. Reddy, P. V. R. R. Reddy, and T. a. J. Reddy, "Finite element analysis of the effect of coefficient of friction on the drawability," *Tribol. Int.*, vol. 43, no. 5–6, pp. 1132–1137, 2010.
- [128] W. M. Garrison and N. R. Moody, "Ductile fracture," *J. Phys. Chem. Solids*, vol. 48, no. 11, pp. 1035–1074, 1987.
- [129] R. A. Lingbeek, T. Meinders, and A. Rietman, "Tool and blank interaction in the cross-die forming process," *Int. J. Mater. Form.*, vol. 1, no. SUPPL. 1, pp.

- 161–164, 2008.
- [130] A. Carpinteri, “Plastic flow collapse vs . separation collapse ( fracture ),” *Matériaux Constr.*, vol. 16, 1983.
- [131] R. Neugebauer, K. D. Bouzakis, B. Denkena, F. Klocke, A. Sterzing, A. E. Tekkaya, and R. Wertheim, “Velocity effects in metal forming and machining processes,” *CIRP Ann. - Manuf. Technol.*, vol. 60, no. 2, pp. 627–650, 2011.
- [132] C. C. Tasan, J. P. M. Hoefnagels, C. H. L. J. ten Horn, and M. G. D. Geers, “Experimental analysis of strain path dependent ductile damage mechanics and forming limits,” *Mech. Mater.*, vol. 41, no. 11, pp. 1264–1276, 2009.
- [133] S. J. H. Z.T. Zhang, “Mathematical Modeling in Plane Strain Bending,” *SAE Tech. Pap.*, 1997.
- [134] T. Zhang, K. Zhou, and Z. Q. Chen, “Strain rate effect on plastic deformation of nanocrystalline copper investigated by molecular dynamics,” *Mater. Sci. Eng. A*, vol. 648, pp. 23–30, 2015.
- [135] U. S. Dixit, S. N. Joshi, and J. P. Davim, “Incorporation of material behavior in modeling of metal forming and machining processes: A review,” *Mater. Des.*, vol. 32, no. 7, pp. 3655–3670, 2011.
- [136] D. Anderson, S. Winkler, A. Bardelcik, and M. J. Worswick, “Influence of stress triaxiality and strain rate on the failure behavior of a dual-phase DP780 steel,” *Mater. Des.*, vol. 60, pp. 198–207, 2014.
- [137] M. K. and M. M. Rahman, “Fatigue Life Estimation Based on Continuum Mechanics Theory with Application of Genetic Algorithm,” *Int. J. Automot. Mech. Eng.*, vol. 11, no. June, pp. 2586–2598, 2015.
- [138] E. E. T. S. and E. C. C. G.M. Domínguez Almaraz, M. Guzmán Tapia, “Fatigue life prediction based on macroscopic plastic zone on fracture surface of AISI-SAE 1018 steel,” *Int. J. Automot. Mech. Eng.*, vol. 1, pp. 29–37, Nov. 2010.
- [139] K. Hariharan and C. Balaji, “Material optimization: A case study using sheet metal-forming analysis,” *J. Mater. Process. Technol.*, vol. 209, no. 1, pp. 324–331, 2009.
- [140] H. Jong, “International Journal of Mechanical Sciences. The forming limit diagram of ferritic stainless steel sheets : Experiments and modeling,” vol. 64, pp. 1–10, 2012.